EVALUATION OF *OPUNTIA FICUS INDICA* AS AN ECONOMIC ADSORBENT FOR ANIONIC RED BEMACID DYE FROM AQUEOUS SOLUTION

AIDA FEKAOUNI,[*,**] GHANIA HENINI[*,***] and YKHLEF LAIDANI[*,**]

[*]*Department of Process Engineering, Faculty of Technology, University Hassiba Ben Bouali, Chlef, Algeria*
[**]*Laboratory of Plant Chemistry, Water and Energy, Faculty of Technology, University Hassiba Ben Bouali of Chlef, Chlef, Algeria*
[***]*Laboratory of Water and Environment Research, Faculty of Technology, University Hassiba Ben Bouali of Chlef, Chlef, Algeria*
✉ *Corresponding author: A. Fekaouni, afekaouni04@gmail.com*

Opuntia ficus indica cladodes (OFIC) were used as an adsorbent for the removal of anionic Bemacid Red (RB) dye from an aqueous solution. The study was performed in a batch reactor under different experimental conditions. The adsorption process was very fast during the first 60 min of phases' contact at 25 °C, the adsorbent being characterized by an adsorption capacity of 16.721 mg/g at pH 2. The experimental data fitted very well with the pseudo-second-order kinetic model ($R^2 = 0.994$), and the Langmuir, Freundlich, Temkin and Dubinin-Radushkevich adsorption models were applied to describe the adsorption equilibrium isotherms. The thermodynamic parameters: enthalpy (-20.739 kJ/mol), entropy (-0.226 kJ/K.mol) and the Gibbs free energy (-14 to -13.557 kJ/mol) were determined over the selected temperature range (25° to 45 °C). The adsorption using the studied system (OFI cladodes/RB) proved to be an exothermic and spontaneous process.

Keywords: *Opuntia ficus indica* cladodes, Red Bemacid dye, adsorption, kinetics, isotherm model

INTRODUCTION

The modern world has witnessed environmental changes resulting from the development of industrial diversity and energy resources, especially water, to meet the demands of the growing population. Most industrial residues are effluents loaded with contaminating agents that may cause environmental pollution. Among industrial effluents, colored effluents produced by large industrial activities, such as dying of leather, paper, textiles, wool, silk, plastics, as well as in cosmetic, food and pharmaceutical industries,[1] are considered a threat to ecosystems.

There are several different classes of organic synthetic dyes. One of the classifications of dyes is based on the charge the molecule carries. Thus, they are classified as anionic (acid dyes), cationic (basic dyes), reactive dyes, azoic dyes and several more types. Acid dyes have sulfonate or carboxylate groups, which distinguish them as soluble in water. They allow dyeing animal fibers (wool and silk) and some modified acrylic fibers (nylon, polyamide) in slightly acidic bath.[2-3] Almost a quarter of these dyes remain unfixed and are discharged into wastewater, posing threats to aquatic species, including animals and plants, but also to humans.[4-5] Dyes can reduce sunlight transmission through water and thus block photosynthesis in aquatic plants. Moreover, these compounds are difficult to biodegrade and many of them are toxic, mutagenic and carcinogenic, causing disorders to humans in the digestive, reproductive, nervous system and liver function.[6]

There are several methods used to remove solids and decolorize effluents, such as coagulation and flocculation, electroflocculation, membrane filtration, advanced oxidation, ozonation, ion exchange, reverse osmosis, biodegradation, electrochemical methods, electrocoagulation and adsorption.[7-12] Among these, adsorption is preferred as an economic and efficient method. It has many advantages

compared the other methods, such as less susceptibility to toxic chemicals, high performance and wide pH range.[13]

In this context, there is much research concerning adsorptive materials, especially those made from inexpensive, abundant and locally available raw materials. Thus, many researchers throughout the world have focused their efforts on developing novel materials as biosorbents with high adsorptive capacity and low cost, and on optimizing the adsorption process. These materials are derived from forest wastes and agricultural residues, such as *Luffa cylindrica*, coconut shells, *Aloe vera*, *Pisum sativum* peels, *Opuntia ficus indica* cactus,[14-18] orange peel[1] and others.

The aim of the present study has been to prepare a biosorbent from *Opuntia ficus indica* cladodes (OFIC) in order to remove Bemacid Red (RB) dye from aqueous solution by adsorption. *Opuntia ficus indica*, also known as prickly pear, is a species of cactus, belonging to the family of *Cactaceae*.[19] It is widely distributed in Mexico, being the most widespread cactus species, but also the most commercially important one, in Latin America, South Africa and the Mediterranean area.[20] The sorption capacity of *Opuntia ficus indica* cladodes towards RB dye has been investigated and the influence of solution pH, contact time, initial dye concentration and amount of adsorbent on the efficiency of adsorption was determined. Four isotherm models, namely, the Langmuir, Freundlich, Temkin and Dubinin-Radushkevich ones, were analyzed to find the best fit to the experimental data. The *Opuntia ficus indica* adsorbent was characterized both before and after adsorption using Fourier transform infrared spectroscopy (FT-IR), X-ray diffraction (XRD) and micro X-ray fluorescence spectrometry (μXRF).

EXPERIMENTAL
Preparation of adsorbent

Cladodes of *Opuntia ficus indica*, a locally available plant, were collected in the north of Algeria and used as adsorbent in this study. The cladodes were washed with distilled boiling water for 15 min, then were placed in a solution of 12% NaOH for 15 min, washed again with tap water and finally dried for 24 hours. They were whitened with 12% bleach for 90 min at ambient temperature, after which were rinsed with distilled water several times. The OFIC were oven dried at 60 °C for 24 hours, then crushed and sifted.

The obtained samples were considered ready for the adsorption study.

Preparation of adsorbate

Red Bemacid (RB) dye is anionic, its solubility in water is of 25 g/L, and the maximum adsorption length λ_{max} = 504 nm. The dye was provided by Soitex Tlemcen, Algeria, and its chemical composition is not disclosed by the company. Stock solutions were prepared by dissolving precise amounts of the dye in distilled water to give a concentration of 1 g/L. The initial pH of the dye solution was adjusted by adding dilute solutions of 0.1N HCl or 0.1N NaOH.

Characterization techniques

The *Opuntia ficus indica* cladodes (OFIC) were characterized before and after adsorption by Fourier transform infrared spectroscopy, using a Prestige-21 FTIR, Shimadzu, Japan. The spectra were recorded by scanning from 400 cm^{-1} to 4000 cm^{-1}. The elemental composition of OFIC was determined by micro X-ray fluorescence spectrometry (μXRF). X-ray diffraction (XRD) analyses were carried out using an APD 2000 model with Cu-Kα irradiation (λ = 1.540598 Å).

Adsorption experiments

For establishing the adsorption isotherm, a series of flasks containing a volume (V = 300 mL) of adsorbate (RB dye) solution of known concentration (20, 30, 50, 70, 80 and 100 mg/L) and a mass (0.5 to 5 g) of the adsorbent of well-defined size (d$_p$ (mm) ≤ 0.15), were placed in a water bath fitted with a stirrer, at different temperatures (25, 35 and 45 °C), with various initial solution pH (2 to 10). For a given contact time, until the adsorption equilibrium was reached, samples were collected and filtered for UV-visible analysis, using a UV-1280 spectrophotometer from Shimadzu. Adsorption kinetic experiments were used to investigate the effect of contact time and determine the kinetic parameters. For these tests, 1 g of OFIC was added to 300 mL of RB dye solutions with different initial concentrations. The mixture was agitated on an electromagnetic stirrer at 700 rpm. At predetermined time intervals (0-120 min), 10 mL samples were taken out and filtered. The same method was used to determine the residual RB dye concentration. Each measurement of RB dye concentration was repeated three times.

The adsorbed dye amount at time t, q$_t$ (mg/g), and the percent of dye removal, R (%), were calculated by the following equations:

$$q_t = \frac{(C_0 - C_t)\,V}{m} \tag{1}$$

$$R\,(\%) = \frac{(C_0 - C_t)}{C_0} \cdot 100 \tag{2}$$

where C_0 and C_t (mg/L) are the concentrations of the RB dye solution at the initial and time t (min),

respectively; V is the volume of adsorbate (L) and m is the mass of adsorbent (g).

Adsorption isotherms

The Langmuir isotherm model is based on the assumption that the maximum amount of solute is adsorbed on the surface of an adsorbent, with the same energy, without interaction between adsorbed molecules, forming only one layer.[21] The general form of the Langmuir isotherm is:

$$\frac{C_e}{q_e} = \frac{1}{q_m K_L} + \frac{C_e}{q_m} \tag{3}$$

where q_e is the amount of dye adsorbed per unit mass of adsorbent (mg/g), C_e is the equilibrium concentration of dye in the solution (mg/L), K_L is the Langmuir constant (L/mg) and q_m is the maximum adsorption capacity (mg/g).

The adsorption viability can be determined from the dimensionless separation factor, also called the equilibrium parameter,[22] R_L, defined using Equation (4). Its value indicates the type of isotherm: irreversible ($R_L = 0$), favorable ($0 < R_L > 1$), linear ($R_L = 1$) or unfavorable ($R_L > 1$).[23]

$$R_L = \frac{1}{1 + K_L C_0} \tag{4}$$

The Freundlich isotherm considers multilayer adsorption accompanied by heterogeneous surface energy systems with interactions between adsorbed molecules. The Freundlich empirical model is represented by:

$$Ln(q_e) = Ln(k_F) + \frac{1}{n_F} Ln(C_e) \tag{5}$$

where K_F (mg g^{-1}(Lmg)$^{-(1/nF)}$) is the Freundlich constant and $(1/n_F)$ the heterogeneity factor, related to the capacity and the biosorption intensity.

The Temkin isotherm model assumes that the heat of adsorption of all molecules on the layer should decrease linearly with the coverage. This model also allows specifying the thermodynamic conditions linked with the adsorption process. The linear form of the Temkin equation is:[24]

$$q_e = \frac{RT}{B_T} Ln\, K_T + \frac{RT}{B_T} Ln\, C_e \tag{6}$$

where B_T is the Temkin constant related to the heat of biosorption (J/ mol), K_T – the Temkin isotherm constant (L/g). R (8.314 J/mol K) is the universal gas constant and T (K) is the absolute solution.

The Dubinin–Radushkevich isotherm assumes that the adsorbent surface is not homogeneous and can be used to estimate the properties of apparent porosity and free energy of the adsorbent. This model is employed to specify the nature of the adsorption process through physisorption or chemisorption. The linear form of this model is described as:

$$Lnq_e = Lnq_m - \beta\, \varepsilon^2 \tag{7}$$

where q_e is the amount of adsorbed dye per adsorbent mass (mg/g), q_m (mg/g) is adsorption capacity, β – the activity coefficient pertinent to the mean adsorption energy and ε – the Polanyi potential, which can be calculated through:

$$\varepsilon = RT\, Ln\left[\left(1 + \frac{1}{C_e}\right)\right] \tag{8}$$

The maximum adsorption energy, E (kJ/mol), provides information about the adsorption process. If the value of E is between 8 and 16 kJ/mol, the adsorption is a chemical process; however, if E <8 kJ/mol, the process occurs physically. It is determined using the following equation:

$$E = \frac{1}{\sqrt{2\beta}} \tag{9}$$

Adsorption thermodynamics

There are thermodynamic parameters that the researchers rely on to describe the adsorption phenomenon. The amount of entropy is the measure of the molecular disorder that must be considered, especially the energy factors, in order to determine the processes that will occur spontaneously.[25] The Gibbs free energy change, ΔG^0, is the fundamental criterion of spontaneity. The value of ΔG^0 can be determined from the following equation:

$$\Delta G^0 = -RT\, Ln(K_d) \tag{10}$$

where $K_d = q_e/C_e$ is the distribution coefficient, R is the gas constant (8.314 J/mol K), and T is the absolute temperature.

A convenient form of the Van't Hoff equation relates K_d to the standard enthalpy and entropy changes of adsorption, ΔH^0 and ΔS^0 respectively.[26]

$$\Delta G^0 = \Delta H^0 - T\Delta S^0 \tag{11}$$

Equation (11) can be written as:[27]

$$Ln(\rho K_d) = \frac{\Delta S^0}{R} - \frac{\Delta H^0}{R} \cdot \frac{1}{T} = -\frac{\Delta G^0}{R} \cdot \frac{1}{T} \tag{12}$$

where ρ is the density of water (g/L), the values of ΔH^0 and ΔS^0 can be determined from the slope and the intercept of the plot between Ln (ρK_d) vs (1/T).

Error analysis

Non-linear isotherm analysis can be used to estimate isotherm data correlation and it is the best method for describing adsorption isotherms, proving the best fitting isotherm model, in contrast to linear analysis, which is insufficient for estimating the isotherm data. In this study, three non-linear error functions were used, as described below.

Chi-square test (χ^2)

This function is based on the sum of the squares of the differences between the experimental and the calculated data, with each square difference divided by

its corresponding values. It is used to find out how closely experimental data fit to calculated data, and helps to find out the significance of the difference in calculated and experiment data. A small chi-square value indicates no differences between calculated and experimental data. χ^2 can be represented by the following equation:[28]

$$\chi^2 = \sum_{i=1}^{N} \frac{\left(q_{e(cal),i} - q_{e(\exp),i} \right)^2}{q_{e(\exp),i}} \tag{13}$$

where $q_{e(cal)}$ (mg/g) is the equilibrium capacity obtained by calculation from the isotherm models (Langmuir, Freundlich, Temkin and Dubinin–Radushkevich) and $q_{e(\exp)}$ (mg/g) is the equilibrium capacity determined from the experimental data, N is number of experimental data points.

Sum of squares error (SSE)

The sum of squares for error is the most widely used error function. It is expressed by:[29]

$$SSE = \sum_{i=1}^{N} \left(q_{e(cal),i} - q_{e(\exp),i} \right)^2 \tag{14}$$

Sum of absolute error (SAE)

This error function will allow providing better fit for high concentration data. It is given by the following equation:[30]

$$SAE = \sum_{i=1}^{N} \left| q_{e(cal),i} - q_{e(\exp),i} \right| \tag{15}$$

Sum of normalized error (SNE)

Each error function allows producing a different set of parameters for each isotherm.[30] In this study, the method called sum of normalized error (SNE) was used to evaluate the best error function for selecting the isotherm model and the calculated isotherm parameters. The calculation process for the sum of normalized errors involves the following steps: 1. Selection of an isotherm model and error function, and determination of the adjustable parameters which minimize the error function; 2. Determination of the values for all other error functions for that isotherm parameter set; 3. Computation of the other parameter sets associated with their error function values; 4. Normalization and selection of the maximum parameter sets with respect to the largest error measurement; 5. Lastly, summation of all these normalized errors for each parameter set.

RESULTS AND DISCUSSION
Physicochemical characterization of the adsorbent

The physicochemical characteristics of OFIC were determined and the results are presented in Table 1. According to the data, OFIC exhibits high volatile matter content, but low ash content.

This can be explained by the composition of the plant: as OFIC is not a woody plant, it is rich in cellulose and hemicelluloses, but with low lignin content. According to previous reports in the literature,[31] *Opuntia ficus indica* contains 64.5% holocellulose, of which 53.6% cellulose, only 4.8% lignin, and 5.5% ash content. It is known that while lignin is the main source of carbon, cellulose and hemicelluloses contribute mostly to the production of volatile matter.

The FTIR spectra of OFIC recorded before and after the adsorption are illustrated in Figure 1. It reveals a wide band at the wavelength of 3436 cm^{-1}, which is assigned to the stretching vibration of the bound OH hydroxyl groups (carboxyl, aromatic and aliphatic),[32] the hydroxyl groups are present in the primary components of wood and non-wood plants: cellulose, hemicelluloses and lignin.[33] The band observed at about 2921 cm^{-1} represents the aliphatic C-H elongation vibration, the peak at about 1638 cm^{-1} corresponds to the C=C ketone elongation vibration. The band around 1059 cm^{-1} is assigned to C-O elongation vibration of an ester, ether, carboxylic acid or alcohol. The band at 666 cm^{-1} may be due to the C-Br bond extension. It can be noted that the results of the spectroscopic analysis for the cladodes before and after the adsorption are the same, except for the peak at 2354 cm^{-1} representing the C≡C bond. This peak disappeared after adsorption and this result may be due to its interaction with RB dye and the dissolution of the triple bond.

The results of elemental analysis by μXRF of both OFIC and RB dye are shown in Figures 2 and 3, respectively. According to Figure 2, OFIC contains high amounts of Cl and Ca, and a small amount of Si. The presence of Cl is due to the bleaching agent used; also, it proves that washing did not completely remove chloride from the surface of OFIC. The composition of RB dye in Figure 3 shows the presence of S and Cl in higher amounts, compared to Si.

The X-ray diffraction analysis of OFIC before and after adsorption are compared in Figure 4. Before adsorption (OFIC raw), the pattern shows the presence of crystalline and amorphous regions with two main peaks at 15.67° and 22.86°, respectively. The OFIC loaded with RB dye exhibits two peaks related to the amorphous and crystalline structure at 15.60° and 22.48°, respectively. Most researchers have established that cellulosic materials have peaks around 20° to 23°, and the intensity is higher than that of the

peaks around 15°.[33-34] The peaks at 22.86° and 22.48° are assigned to the crystal lattice of OFIC; crystallization in an orthorhombic unit cell has been reported ($B_{12}H_{16}$).

Table 1
Physical characteristics of the material (OFIC)

Materials	OFIC
Moisture content (%)	7.7
Ash content (%)	4.033
Volatile compounds (%)	88.267
Apparent density (g/cm^3)	1.510
Swelling (%)	13.330
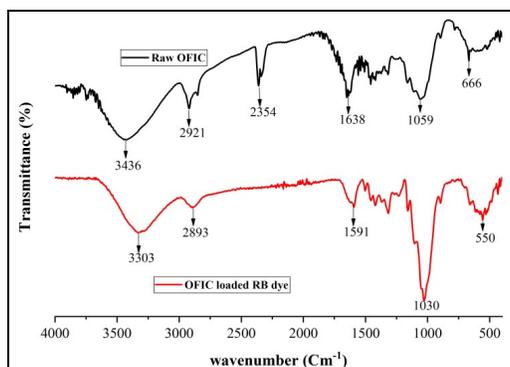
Figure 1: FT-IR spectra of raw OFIC and OFIC loaded with RB dye
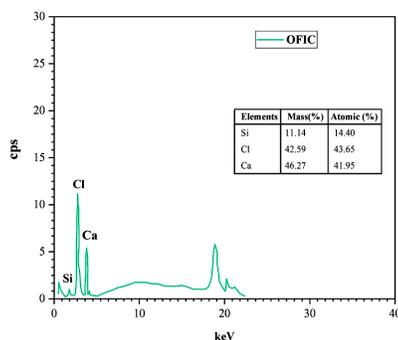
Figure 2: Micro X-ray fluorescence spectrometry (µXRF) of OFIC
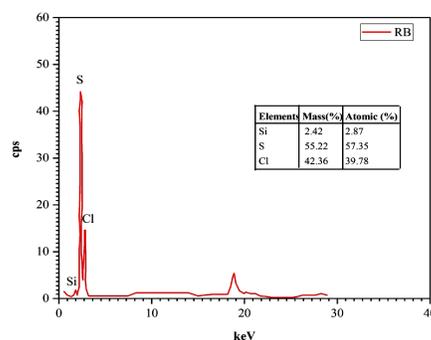
Figure 3: Micro X-ray fluorescence spectrometry (µXRF) of RB dye
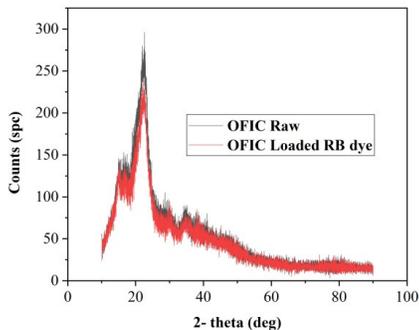
Figure 4: X-ray diffraction patterns of raw OFIC and OFIC loaded with RB dye
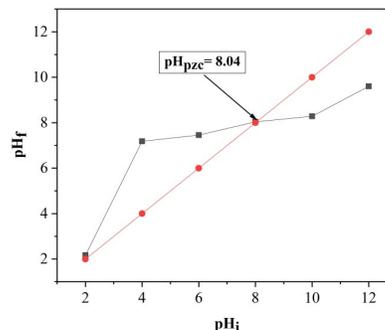
Figure 5: Determination of pH_{pzc} for OFIC

Table 2
Degree of crystallinity and amorphous content of OFIC raw and loaded with RB dye

Samples	Degree of crystallinity (DC, %)	Amorphous content (weight, %)
OFIC raw	61.44	38.56
OFIC loaded with RB	41.45	58.55

The degree of crystallinity (DC) and amorphous content were calculated by using Match type data processing software and the results obtained are presented in Table 2. Thus, the DCs of OFIC raw and loaded with RB dye were observed as 61.44% and 41.45%, while the amorphous content – as 38.56% and 58.55%. It was observed that the DC of the biosorbent decreased after dye adsorption, while its amorphous content increased. These results can be explained by the integration of RB dye in the crystalline structure of the biosorbent during the adsorption process, therefore it becomes more amorphous.

Zero charge point (pH$_{PZC}$)
The pH$_{pzc}$ of the used OFIC was determined as follows: in a series of beakers, 50 mL of NaCl (0.05 M) was added, the pH$_i$ of each was adjusted to precise values of 2 to 12 by the addition of 0.1 M NaOH and 0.1 M HCl with 0.5 g of adsorbent. The suspensions were maintained under constant stirring at room temperature for 48 hours to determine the final pH. The pH$_{pzc}$ is defined as the point where the curve pH$_i$ versus pH$_f$ crosses the line pH$_i$ = pH$_f$. Figure 5 shows the curve that gives the pH of zero charge (pH$_{pzc}$).

Adsorption experiments
Effects of contact time
Contact time is considered as an important factor to consider when observing the mechanism and kinetics of the absorption phenomenon.[35] The effects of contact time on the adsorption of RB dye from aqueous solution onto OFIC (dp ≤ 0.15 mm) were analyzed and the results are presented in Figure 6. The adsorption is fast at the beginning of the process until t = 10 min, when it gradually slows down until reaching the equilibrium. The contact time required to establish the adsorption equilibrium was approximately 60 min in the present study. This result is an agreement with those reported by some other previous research carried out on the adsorption of dyes onto various biosorbents under different conditions.[36-37]

Effects of adsorbent concentration
A series of experiments have been performed with different adsorbent concentration (0.5, 1, 1.5, 2, 3, 4 and 5 g per 300 mL of dye solution) with the aim to establish the effect of increasing the amount of adsorbent on the adsorption capacity and to determine the optimal adsorbent concentration. Figure 7 shows that the adsorbed amount of RB dye increased significantly till equilibrium as the amount of OFIC per 300 mL dye solution was increased. Indeed, as the adsorbent concentration rose from 0.5 to 5 g per 300 mL of solution, the removal of RB dye enhanced from 49.69% to 71.42%, thus, the adsorption capacity decreased from 20.87 to 3 mg/g for an initial concentration of 70 mg/L RB dye. The increase in the rate of retention of RB dye as a function of the increase in adsorbent amount is mainly due to a consequent increase in the adsorption surface area, thus offering more active sites for the retention of the pollutant molecule. On the other hand, it can be remarked that the quantity of adsorbed dyes decreases with increasing the mass of the adsorbent, possibly explained by random distribution of the dye molecules at the level of the adsorption surface of each particle. The same trend has been reported for the adsorption of textile dyes onto *Posidonia oceanica* fibers, where a significantly higher removal of dye (from 26% to 91%) was achieved increasing the adsorbent concentration from 1 to 50 g/L.[38]

Initial dye concentration effect
The influence of the initial concentration of RB dye on the adsorption capacity of OFIC was studied for 20, 30, 50, 70 and 100 mg/L dye concentrations. The tests were carried out at pH = 5.68 and a temperature of 25 °C. The results presented in Figure 8 show an increase in the amount of dye adsorbed as a function of the rising initial dye concentration. Indeed, the biosorption capacity records an increase from 1.94 to 12.45 mg/g, respectively, for concentrations from 20 to 100 mg/L dye. This behavior is explained by the

fact that the higher the concentration of RB dye, the higher the number of ions in the solution available for retention, implying higher adsorption. The same phenomenon was also reported for dye adsorption onto de-oiled algal biomass, when researchers found that the methylene blue dye adsorption increases with increasing concentration of the dye in the solution. After reaching the methylene blue dye concentration of 2000 mg/L, the adsorbed amount gradually reached a plateau, with no further increases being recorded.[39]
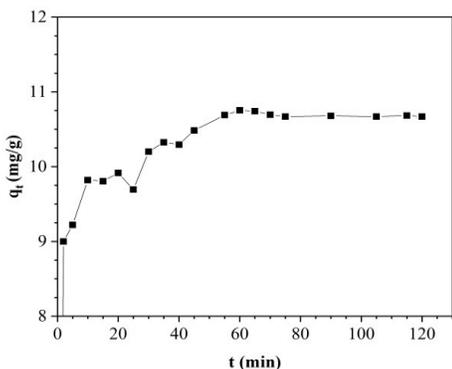
Figure 6: Effect of contact time on RB dye removal by OFIC adsorbent: $C_{adsorbent}$ = 3.33g/L, C_0 = 70 mg/L RB dye, T = 25 °C, pH = 5.68, d_p (mm) ≤ 0.15 and ω = 700 rpm
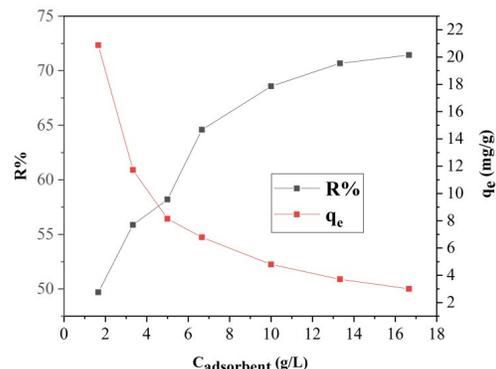
Figure 7: Effect of adsorbent concentration on RB dye removal by OFIC adsorbent: C_0 = 70 mg/L RB dye, adsorption time = 60 min, d_p (mm) ≤ 0.15 and T = 25 °C
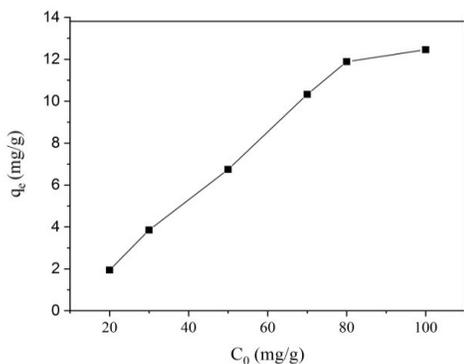
Figure 8: Effect of initial RB concentration on adsorption capacity of OFIC adsorbent: pH = 5.68, $C_{adsorbent}$ = 3.33 g/L, adsorption time = 60 min, T = 25 °C, d_p (mm) ≤ 0.15 and ω = 700 rpm
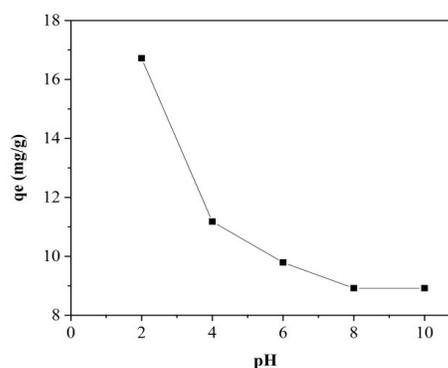
Figure 9: Influence of pH on the adsorption of RB dye onto OFIC adsorbent: $C_{adsorbent}$ = 3.33 g/L, C_0 = 70 mg/L RB dye, T = 25 °C and adsorption time = 60 min
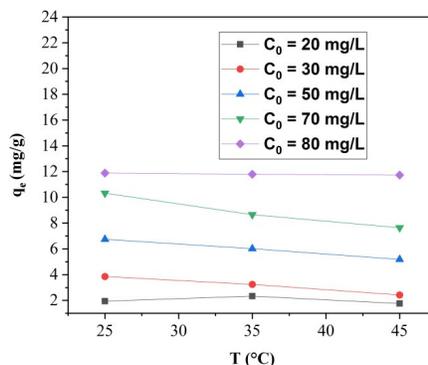
Figure 10: Effect of temperature on RB dye removal by OFIC adsorbent: $C_{adsorbent}$ = 3.33 g/L, adsorption time = 60 min, d_p (mm) ≤ 0.15, pH = 2

Influence of pH

The initial pH of the dye solution is an important operational parameter that must be considered during an adsorption study. The effect of this factor on the adsorption capacity of the OFIC biosorbent was analyzed over a pH range from 2 to 10, as shown in Figure 9.

The results showed a decrease in the adsorbed amount of RB with rising pH of the solution. The adsorption of RB can be envisaged as the electrostatic interaction between the negative charge of the dye and the positive charge of the adsorbent material, which may be reinforced by the polarity of the dye molecule. This interaction decreases when the pH increases towards the pH$_{PZC}$ (pH$_{PZC}$ = 8.07) of OFIC, because the surface charge of the OFIC gradually becomes nil, the decrease of adsorption is explained by the electrostatic repulsion between the dye molecule (negative charge) and the adsorbent surface, which becomes increasingly negative when the pH > 8.07. From the results obtained, the most favorable pH for the removal of RB is pH = 2, when an adsorption capacity of 16.72 mg/g was reached after 60 min. This value is much higher than those achieved for other materials previously reported as adsorbents for the removal of dyes, for example, the adsorption capacity of 3.89 mg/g for 1 g of *Posidonia oceanica* fibers and 50 mL of dye solution was recorded at pH = 2[38] and 5.97 mg/g adsorption was achieved using 20 mg of cellulose per 50 mg of dye solution at pH = 2.[40]

Temperature effect

Temperature is one of the most important factors affecting the adsorption of dyes from aqueous solutions. The effect of temperature on the adsorption isotherm was studied by carrying out a series of tests at 25, 35 and 45 °C, as shown in Figure 10. As may be noticed, the adsorption capacity decreases with increasing temperature. This phenomenon suggests that the reaction is exothermic, thus, a temperature increase is unfavorable for the adsorption mechanism. Similarly, the exothermic nature of the adsorption process has been found for other adsorbent systems.[14,41]

Kinetics of dye adsorption

The data of RB adsorption kinetics on OFIC were fitted to the pseudo-first-order[42] and the pseudo-second-order[43] kinetic models in order to describe the adsorption mechanism. These are the most commonly used models to correlate the

experimental data. The Lagergren's pseudo-first-order equation is the following:

$$\frac{dq_t}{dt} = k_1(q_e - q_t) \qquad (16)$$

The linear form of this equation is:

$$Ln(q_e - q_t) = Lnq_e - k_1 t \qquad (17)$$

where q$_e$ is the amount of dye biosorbed at equilibrium (mg/g), q$_t$ (mg/g) is the amount of dye biosorbed at time t, K$_1$ is the first-order rate constant (min^{-1}) and t is adsorption time (min). Hence, a linear trace is expected between the two parameters, Ln (q$_e$-q$_t$) and t, provided that the biosorption follows first-order kinetics. The values of k$_1$ and q$_e$ can be determined from the slope and intercept, as shown in Figure 11.

The pseudo-second-order kinetic model can be represented in the following form:[44]

$$\frac{t}{q_t} = \frac{1}{k_2 q_e^2} + \frac{1}{q_e} t \qquad (18)$$

where q$_e$ is the amount of dye adsorbed at equilibrium (mg/g) and K$_2$ is the rate constant of pseudo-second-order adsorption (g/mg min). The values of K$_2$ and q$_e$ can be determined experimentally from the slope and intercept of the plot t/q$_t$ versus t. The K$_2$ and q$_e$ values under different conditions were calculated and listed in Table 3.

The linear plots of t/qt versus t in Figure 12 show a good agreement between the experimental (q$_{e,exp}$) and the calculated (q$_{e,cal}$) data (Table 3). Also, the correlation coefficients for the pseudo-second-order kinetic model (R^2) are greater than 0.996, indicating the applicability of this kinetic equation to describe the adsorption process of RB onto OFIC and the fact that the process is controlled by physisorption.[45]

Adsorption isotherms

The analysis of isotherm models allows describing the interaction and the degree of affinity between solutes and adsorbents. Each model has its own parameters that enable deeper understanding of the adsorption mechanisms and adsorbent surface properties. We have selected four most common models used to investigate the adsorption mechanism: the Langmuir, Freundlich, Temkin and Dubinin-Radushkevich ones. Each of these models either offers a unique description of the phenomenon or complements another one of them. The experimental results of this study have been fitted to these models.
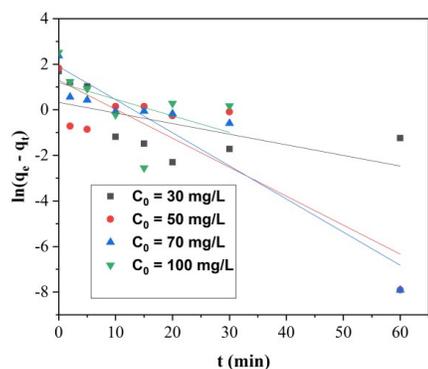
Figure 11: Linearization of the pseudo-first-order kinetic model for RB/OFIC at T = 25 °C
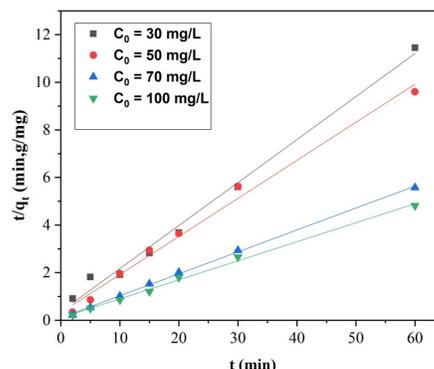
Figure 12: Linearization of the pseudo-second-order kinetic model for RB/OFIC at T = 25 °C

Table 3
Kinetic parameters for the removal of RB by OFIC

C_i (mg/L)	$q_{e,exp}$ (mg/g)	Pseudo-first-order model			Pseudo-second-order model		
		$q_{e,cal}$ (mg/g)	K_1 (g/mg.min)	R^2	$q_{e,cal}$ (mg/g)	K_2 (g/mg.min)	R^2
30	5.4315	1.3862	0.0466	0.354	5.5340	0.0897	0.991
50	6.2526	3.6513	0.1272	0.739	6.2539	0.0788	0.990
70	10.7526	6.6932	0.1454	0.884	10.8577	0.0774	0.999
100	18.4736	2.0503	0.0237	0.104	12.5156	0.0615	0.996

The obtained isotherm parameters corresponding to the Langmuir, Freundlich, Temkin and Dubinin–Radushkevich (D-R) models are given in Table 4 (with mathematical adjustments of experimental data to equilibrium). The adsorption isotherms describe the relationship between RB dye and the OFIC adsorbent used for its removal from solution. Table 4 provides the values of different isotherm constants, R^2 (correlation coefficient), χ^2 chi-square, sum of squares for error (SSE) and sum of absolute error (SAE). Based on the correlation coefficient R^2, chi-square (χ^2), SSE and SAE for various temperature (25, 35 and 45 °C), it follows the Freundlich and Temkin models are the most appropriate for describing satisfactorily the present adsorption phenomenon (R_F^2 = 0.992), providing the best linear correlation coefficient and lower values of χ^2, SSE and SAE. However, comparing the results for the two models, it is clear that the Freundlich model provides a better fit to equilibrium data than the Temkin isotherm model for various temperatures. In addition, the relation between R_L and C_0 (mg/L) according to the Langmuir isotherm for RB dye adsorption onto OFIC is shown in Figure 13. The values of

R_L for the initial RB dye concentrations and various temperatures (25, 35 and 45 °C) are found in the range $R_L > 1$, which suggests unfavorable adsorption of RB dye onto OFIC under the conditions of the experiments.

The method of linear transformation of the isotherm model with the highest values of the linear regression coefficient is not sufficient to choose the appropriate isothermal model and the calculated isotherm parameters for the adsorption system RB/OFIC. The nonlinear approach of the isotherm models used the three-error function to fit the equilibrium data and to determine the isotherm parameters, using the Solver add-in in Microsoft Excel. The calculated values of the parameters and the error analysis for various temperatures (25 °C, 35 °C and 45 °C) are illustrated in Tables 5, 6, 7 and 8.

The values of the Sum of Normalized Errors (SNE) were used to evaluate the best error function for selecting the most suitable isotherm model and the calculated isotherm parameters. The values shown in the tables indicate the minimum values of SNE for an appropriate error function, according to the results in Table 5.

Table 4
Data derived from various isotherm plots for adsorption of RB onto OFIC

Isotherm	Parameters	Temperature		
		25 °C	35 °C	45 °C
Langmuir	q_m (mg/g)	-7.806	-27.473	-10.341
	K_L (L/mg)	-0.017	-0.006	-0.010
	R^2	0.833	0.829	0.841
	χ^2	0.299	0.035	0.094
	SSE	1.441	0.169	0.333
	SAE	2.130	0.763	0.992
Freundlich	K_F (mg/g)(Lmg)$^{(1/n_F)}$	0.024	0.122	0.046
	$1/n_F$	1.685	1.154	1.342
	R^2	0.999	0.993	0.984
	χ^2	0.039	0.065	0.109
	SSE	0.422	0.367	0.350
	SAE	1.068	1.090	1.092
Temkin	K_T (L/mg)	0.090	0.111	0.087
	B_T (j/mol)	275.032	459.34	506.291
	R^2	0.992	0.960	0.959
	χ^2	0.019	0.548	0.745
	SSE	0.117	2.123	1.774
	SAE	0.657	2.902	2.483
Dubinin-Radushkevich	q_m (mg/g)	14.443	10.503	10.027
	β	7×10^{-5}	4×10^{-5}	5×10^{-5}
	E (Kj/mol)	0.085	0.111	0.1
	R^2	0.999	0.948	0.935
	χ^2	0.120	1.360	2.265
	SSE	0.666	11.512	17.849
	SAE	1.305	5.087	6.701
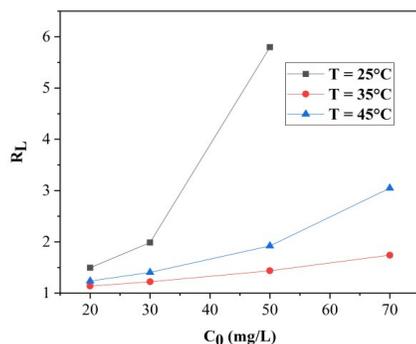
Figure 13: Plot of R_L versus initial RB dye concentration with various temperatures at pH = 2, adsorption time = 60 min, $C_{adsorbent}$ = 3.33 g/L and ω = 700 rpm
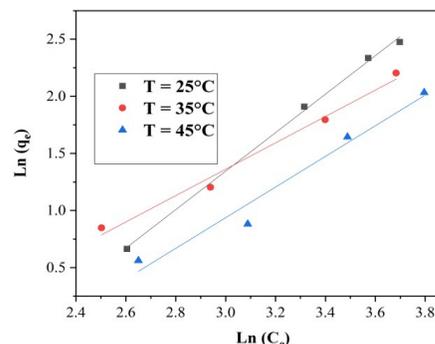
Figure 14: Linearization of Freundlich equation for RB/OFIC adsorption: pH = 2, C_0 = 70 mg/L RB dye, and $C_{adsorbent}$ = 3.33 g/L

It was found that the SAE function provides the best estimation of the parameters for the Langmuir isotherm. The individual constant q_m and K_L for different temperature (25 °C, 35 °C and 45 °C) are significantly different, the error values for the parameters set are greater than the same error determined for the linear form of the

isotherm. These results suggest that the Langmuir isotherm does not offer a good description for the adsorption mechanism of RB dye onto OFIC.

The SSE function provides the best estimation of the parameters for the Temkin model at (25 °C, 45 °C), as can be observed in Table 7. The results show that the non-linear form of the Temkin

isotherm provides a close fit to linear sorption data at the temperatures mentioned. Thus, the non-linear analysis method shows K_T and B_T parameters to be quite consistent and comparable with the values derived by linearization. The SSE parameter set is a better fit than two other error analyses (χ^2, SAE).

Table 5
Non-linear Langmuir isotherm parameters

Method/Error function (parameter set)		
SSE	χ^2	SAE
T = 25 °C		
q_m (mg/g) 1521.93861	791.718863	22.6314111
K_L (L/mg) 0.00016962	0.00029161	0.01541496
SSE 4.23630047	4.1743165	4.19749302
χ^2 1.17566679	1.20068109	1.18013971
SAE 3.35736306	3.38023002	5.15410928
SNE 2.07004446	2.09740388	2.04336801
T = 35 °C		
q_m (mg/g) 0.49297953	330.94049	6.26716986
K_L (L/mg) 0.09853813	0.00062124	0.06006399
SSE 1.83028346	1.02661785	1.0590294
χ^2 0.19945973	0.21653479	0.1983316
SAE 8.51647669	1.72662156	6.94746526
SNE 1.23833133	1.71999138	1.18098126
T = 45 °C		
q_m (mg/g) 440.26313	432.069504	20.0580912
K_L (L/mg) 0.0003588	0.0003374	0.01063229
SSE 1.79359668	1.71011672	1.71626685
χ^2 0.51537716	0.53521896	0.51760122
SAE 2.19384707	2.19340471	3.44823609
SNE 2.05247712	2.02367597	1.64782921

Table 6
Non-linear Freundlich isotherm parameters

Method/Error function (parameter set)		
SSE	χ^2	SAE
T = 25 °C		
K_F (mg/g)(Lmg)$^{(1/n_F)}$ 0.03583489	0.02826419	0.04904845
1/n 1.57114587	1.64271652	1.48509991
SSE 0.353791	0.26251196	0.26251136
χ^2 0.03484105	0.03484158	0.03484102
SAE 0.92193708	0.96867161	0.87801064
SNE 3.08810714	1.30697043	1.33866603
T = 35 °C		
K_F (mg/g)(Lmg)$^{(1/n_F)}$ 0.08557098	0.10128312	0.06756496
1/n 1.26135936	1.21179111	1.32639357
SSE 0.19846554	0.19837503	0.19837491
χ^2 0.05609548	0.05609548	0.05609548
SAE 0.7653756	0.90659945	0.70782621
SNE 1.3325962	1.28068681	1.35950971
T = 45 °C		
K_F (mg/g)(Lmg)$^{(1/n_F)}$ 0.03869955	0.0360899	0.05528448
1/n 1.38964709	1.40998194	1.29842776
SSE 0.28405571	0.26471843	0.26471838
χ^2 0.10780338	0.10795783	0.10780338
SAE 0.80087319	0.79363479	0.71364018
SNE 1.48928982	1.46958155	1.52200223

For the Dubinin-Radushkevich (D-R) isotherm, the SAE function gives the best estimation of the parameters at 25 °C and 35 °C, as revealed by the data in Table 8. The values of the constants q_m and β are significantly different for each error method at a different temperature.

Based on the linear and non-linear results, the Freundlich isotherm is the best suitable model for the adsorption system RB/OFIC. The Freundlich model assumes that the adsorption sites present on the surface are energetically heterogeneous and that the adsorption occurs as a multilayer process. Also, the values of the mean adsorption energy E (Kj/mol) obtained from the Dubinin–Radushkevich model are less than 8 Kj/mol. It indicates that the adsorption process is physical. This is confirmed by the fact that the correlation coefficient decreases with the increase in temperature. These results are in agreement with previous works on biosorption of pollutants.[46] The values of the Temkin model constants

demonstrate that the adsorption of RB dye from aqueous solution onto OFIC has an inverse relationship with the temperature increase.

Table 9 presents a comparison of the maximum biosorption capacity (q_{max}) of RB dye onto OFIC with those reported for other biosorbents in the literature. It is clear that the OFIC used in this work, without any treatment, has a relatively suitable biosorption capacity, compared to other biosorbents in the literature.

Adsorption thermodynamics

Van't Hoff plot analysis was used to determine whether the adsorption of RB dye onto OFIC is an exothermic or endothermic process (Fig. 15). The ΔG^0 values were calculated using Equation (12). The values of ΔG^0, ΔH^0 and ΔS^0 for the biosorption of RB dye onto OFIC at different temperatures 298, 308 and 313 K are given in Table 10.

Table 7
Non-linear Temkin isotherm parameters

Method/Error function (parameter set)			
	χ^2	SSE	SAE
T = 25 °C			
K_T (L/mg)	0.0913108	0.09054824	0.09239547
B_T (j/mol)	278.161229	275.031627	285.532444
χ^2	0.01637048	0.01637048	0.01637048
SSE	0.11738605	0.11738605	0.11738605
SAE	0.63005698	0.63706368	0.62035904
SNE	1.21229275	1.20995787	1.21561148
T = 35 °C			
K_T (L/mg)	0.1212919	0.11074438	0.0955798
B_T (j/mol)	515.399026	459.395333	447.649652
χ^2	0.44643423	0.44643423	0.44643423
SSE	2.12264897	2.12264897	2.12264897
SAE	2.76350916	2.680542	2.9245504
SNE	1.92964527	1.95841931	1.87845407
T = 45 °C			
K_T (L/mg)	0.0948832	0.08694265	0.06841523
B_T (j/mol)	581.289945	506.296085	411.637178
χ^2	0.60181538	0.60181538	2.23302995
SSE	1.77364636	1.77364636	1.77364636
SAE	2.343065	2.44759748	2.6400707
SNE	2.01382665	1.97052794	2.51763978

Table 8
Non-linear Dubinin-Radushkevich (D-R) isotherm parameters

Method/Error function (parameter set)		
SSE	χ^2	SAE
T = 25 °C		
E (Kj/mol)	85.9734019	86.9133241	85.074674
q_m (mg/g)	14.7639898	14.6079408	15.0021159
β	6.7646E-05	6.6191E-05	6.9083E-05
SSE	0.3311851	0.3311851	0.3311851
χ^2	0.03666771	0.03666771	0.03666771
SAE	0.95396292	0.9537952	0.95996609
SNE	1.38560494	1.38567275	1.38319355
T = 35 °C		
E (Kj/mol)	52.6619954	112.299938	49.1058891
q_m (mg/g)	21.325081	10.4718405	26.0465272
β	0.00018029	3.9647E-05	0.00020735
SSE	8.29050877	8.29050876	8.29050877
χ^2	1.29478919	1.29478919	1.29478919
SAE	4.65161836	4.76698142	4.6495265
SNE	1.71725484	1.73116992	1.71700252
T = 45 °C		
E (Kj/mol)	68.3785774	93.9835282	68.3491403
q_m (mg/g)	13.4558793	9.85611806	11.0492721
β	0.00010694	5.6607E-05	0.00010703
SSE	16.5179116	16.5179116	16.5179115
χ^2	1.91559463	1.91559463	1.91559463
SAE	6.32232329	5.94055005	6.43864353
SNE	1.49872636	1.47561368	1.50576843

Table 9
Comparison of maximum biosorption capacity of different absorbents towards dyes

Adsorbents	Adsorbate	q_{max} (mg/g)	pH	Reference
Pisum sativum peels	Alizarin Yellow	2.47	3	R. Rehman et al.[17]
	Murexide	11.04	3	
Orange peel	Direct Red 23	10.72	2	M. Arami et al.[47]
	Direct Red 80	21.05	2	
Aloe vera AV-AC	Red Congo	1850	2	Y. O. Khaniabadi et al.[16]
Bengal gram fruit shell (SP)	Red Congo	22.22	8	L. S. Krishnaab et al.[48]
Raw *Luffa cylindrica*	Methylene Blue	49.46	10	N. Boudechiche et al.[14]
Banana peel powder	Reactive Black 5	49.2	3	V. S. Munagapati et al.[49]
	Congo Red	164.6	3	
Luffa cylindrica activated by NaOH (2%)	Malachite Green	29.4	5	A. Altinişik et al.[50]
Teak leaf litter	Acid Blue 40	80.64	2	E. O. Oyelude et al.[51]
Opuntia ficus indica cladodes	Red Bemacid	16.721	2	Present work

Table 10
Thermodynamic parameters for RB dye adsorption onto OFIC

Temperature (K)	ΔH^0 (kJ/mol)	ΔS^0 (kJ/mol.K)	ΔG^0 (kJ/mol)
298			-14
308	-20.739	-0.226	-13.783
318			-13.557
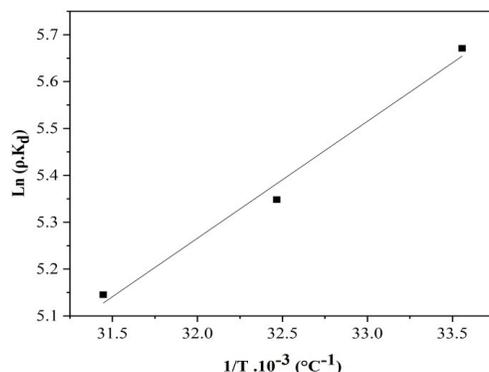
Figure 15: Van't Hoff plot for determining the thermodynamic parameters for RB/OFIC, C_0 = 70 mg/L RB dye

The negative (ΔG^0) values of Gibbs free energy represent that the adsorption is a thermodynamically feasible reaction and is spontaneous in nature.[52] Generally, the change in adsorption enthalpy for physisorption is in the range from 20 to 40 kJ/mol, while for chemisorption it is between 40 and 400 kJ/mol. The ΔG^0 values obtained in this study for the adsorption of RB are <20 kJ/mol, which indicates physical adsorption. The negative ΔH^0 value (-20.739 kJ/mol) shows that the nature of the adsorption is exothermic. The negative ΔS^0 value (-0.226 kJ/mol.K) suggests a decrease in randomness during the adsorption of RB dye onto OFIC. The same phenomenon was observed previously for the adsorption of BM onto *Luffa cylindrica*.[14]

CONCLUSION

In the present research, we have studied the adsorption capacity of cladodes of a Mediterranean plant *Opuntia ficus indica* for the removal of RB dye from aqueous solution. The equilibrium adsorption capacity could be optimized by increasing the amount of adsorbent fiber and the initial dye concentration. Higher adsorption capacity was recorded at a more acid pH. On the other hand, the analysis of the adsorption kinetics has shown that the adsorption phenomenon studied in the present work is better described by the pseudo-second-order model, thus suggesting a possible physical adsorption.

The Sum of the Normalized Errors was used to evaluate the best error function for selecting the most suitable isotherm model and the calculated isotherm parameters. The Freundlich isotherm has demonstrated the best fit to the equilibrium data for the adsorption of RB dye onto OFIC, based on a comparison between the linearized correlation coefficient and non-linear regression data. The thermodynamic parameters described the process of RB dye adsorption onto OFIC as spontaneous and exothermic.

The findings of the present study indicate that OFIC could be employed as a low-cost alternative to commercially available adsorbents for different aqueous treatment systems, aiming to remove anionic dyes from polluted wastewaters.

REFERENCES
[1] M. R. Mafra, I. L. Mafra, D. R. Zuim, É. C. Vasques and M. A. Ferreira, *Braz. J. Chem.*, **30**, 657 (2013), https://doi.org/10.1590/S0104-66322013000300022
[2] M. M. Ayad and A. Abu El-Nasr, *J. Nanostruct. Chem.*, **3**, 2 (2012), https://doi.org/10.1186/2193-8865
[3] H. Benmonsour and O. Boughzala, *J. Water Sci.*, **24**, 209 (2011), https://doi.org/10.7202/1006453ar
[4] K. M. Kifuani, K. A. Kifuani, V. Ph. Noki, L. B. Ilinga, B. G. Ekoko *et al.*, *Int. J. Biol. Chem. Sci.*, **12**, 568 (2018), https://doi.org/10.4314/ijbcs.v12i1.43
[5] M. Saquib and M. Muneer, *Dyes Pigm.*, **56**, 37 (2003), https://doi.org/10.1016/S0143-7208(02)00101-8
[6] B. Lellis, C. Z. Fávaro-Polonio, J. A. Pamphile and J. C. Polonio, *Biotechnol. Res. Innov.*, **3**, 275 (2019), https://doi.org/10.1016/j.biori.2019.09.001
[7] V. Saritha, N. Srinivas and N. V. Srikanth Vuppala, *Appl. Water Sci.*, **7**, 451 (2017), https://doi.org/10.1007/s13201 014-0262-y
[8] H. A. Maddah, A. S. Alzhrani, M. Bassyouni, M. H. Abdel Aziz, M. Zoromba *et al.*, *Appl. Water Sci.*,

150, 1 (2018), https://doi.org/10.1007/s13201-018-0793-8

9 P. Vanessa, A. Andrin, M. LeBechec, S. Lacombe, J. Frayret *et al*., *J. Water Sci*., **30**, 35 (2017), https://doi.org/10.7202/1040061ar

10 G. Moussavi and M. Mahmoudi, *Chem. Eng. Sci*., **152**, 1 (2009), https://doi.org/10.1016/j.cej.2009.03.014

11 M. El Haddad, R. Slimani, R. Mamouni, R. Laamari, S. Rafqah *et al*., *J. Taiwan Inst. Chem. E*., **44**, 13 (2013), https://doi.org/10.1016/j.jtice.2012.10.003

12 O. Ali and S. Mohamed, *Turk. J. Chem*., **41**, 967 (2017), https://doi.org/10.3906/kim-1703-72

13 M. Ganesapillai, A. Venugopal, V. Ananthkrishna and N. Tapankrishna, *Asia-Pac. J. Chem. Eng*., **10**, 438 (2015), https://doi.org/10.1002/apj.1888

14 N. Boudechiche, H. Mokaddem, Z. Sadaoui and M. Trari, *Int. J. Ind. Chem*., **7**, 167 (2016), https://doi.org/10.1007/s40090-015-0066-4

15 K. S. Gbamele, G. P. Atheba, B. K. Dongui, P. Drogui, D. Robert *et al*., *Afr. Sci*., **12**, 229 (2016)

16 Y. O. Khaniabadi, M. J. Mohammadi, M. Shegerd, S. Sadeghi, S. Saeedi *et al*., *Environ. Eng. Manag. J*., **4**, 29 (2017), https://doi.org/10.15171/EHEM.2017.05

17 R. Rehman, T. Mahmud and A. Arshad, *Asian J. Chem*., **27**, 1593 (2015), https://doi.org/10.14233/ajchem.2015.17383

18 A. K. Degbe, M. Koriko, S. Tchegueni, E. Aziable, I. Tchakala *et al*., *J. Mater. Environ. Sci*., **7**, 4786 (2016), https://www.jmaterenvironsci.com/Document/vol7/vol7_N12/505 JMES-2575Degbe.pdf

19 M. P. Griffith, *Am. J. Bot*., **91**, 1915 (2004), https://doi.org/10.3732/ajb.91.11.1915

20 M. Kaur, A. Kaur and R. Sharma, *J. Appl. Pharm. Sci*., **2**, 15 (2012), https://doi.org/10.7324/JAPS.2012.2703

21 S. Mustapha, D. T. Shuaib, M. M. Ndamitso, M. B. Etsuyankpa, A. Sumaila *et al*., *Appl. Water. Sci*., **9**, 142 (2019), https://doi.org/10.1007/s13201-019-1021-x

22 A. A. Khan, R. Ahmad, A. Khan and P. K. Mondal, *Arab. J. Chem*., **6**, 361 (2013), https://doi.org/10.1016/j.arabjc.2010.10.012

23 Z. Zhang, D. Shi, H. Ding, H. Zheng and H. Chen, *Int. J. Environ. Sci. Technol*., **12**, 3351 (2015), https://doi.org/10.1007/s13762-015-0762-9

24 A. U. Itodo and H. U. Itodo, *Life Sci*., **7**, 31 (2010), https://doi.org/10.7537/marslsj070410.05

25 A. Achmad, J. Kassim, T. K. Suan, R. Ch. Amat and T. L. Seey, *J. Phys. Sci*., **23**, 1 (2012), https://jps.usm.my/uncaria-gambir-extract/

26 N. Velinov, S. Najdanović, M. R. Vučić, J. Mitrović, M. Kostić *et al*., *Cellulose Chem. Technol*., **53**, 175 (2019), https://doi.org/10.35812/CelluloseChemTechnol.2019.53.20

27 S. K. Milonjic, *J. Serbian Chem. Soc*., **72**, 1363 (2007), https://doi.org/10.2298/JSC0712363M

28 N. Ayawei, A. N. Ebelegi and D. Wankasi, *J. Chem*., **11** (2017), https://doi.org/10.1155/2017/3039817

29 A. L. Prasada, T. Santhi and S. Manonmani, *Arab. J. Chem*., **8**, 343 (2015), https://doi.org/10.1016/j.arabjc.2011.01.020

30 H. R. Ghaffari, H. Pasalari, A. Tajvar, K. Dindarloo, B. Goudarzi *et al*., *Int. J. Eng. Sci*., **9**, 01 (2017), https://doi.org/10.9790/1813-0609010111

31 F. Mannai, M. Ammar, J. G. Yanez, E. Elaloui and Y. Moussaoui, *Cellulose*, **23**, 2061 (2016), https://doi.org/10.1007/s10570-016-0899-9

32 S. A. Mohtashami, N. Asasian Kolur, T. Kaghazchi, R. Asadi Kesheh and M. Soleimani, *Turk. J. Chem*., **42**, 1720 (2018), https://doi.org/10.3906/kim-1806-71

33 N. Nordine, Z. El Bahri, H. Sehil, R. I. Fertout, Z. Rais *et al*., *Appl. Water Sci*., **6**, 349 (2016), https://doi.org/10.1007/s13201-014-0233-3

34 M. Abbas, *Adsorp. Sci. Technol*., **38**, 464 (2020), https://doi.org/10.1177/0263617420957829

35 D. Chebli, A. Bouguettoucha, T. Mekhalif, S. Nacef and A. Amrane, *Desalin. Water Treat*., **54**, 245 (2015), https://doi.org/10.1080/19443994.2014.880154

36 O. Khelifi, I. Mehrez, W. Ben Salah, F. Ben Salah, M. Younsi *et al*., *Larhyss J*., **28**, 135 (2016), http://larhyss.net/ojs/index.php/larhyss/article/view/464

37 D. B. Kumar and S. Kacha, *J. Water Sci*., **24**, 131 (2011), https://doi.org/10.7202/1006107ar

38 M. Ch. Ncibi, B. Mahjoub and M. Seffen, *J. Environ. Eng. Sci*., **7**, 645 (2008), https://doi.org/10.1139/S08-040

39 R. Maurya, T. Ghosh, Ch. Paliwal, A. Shrivastav, K. Chokshi *et al.*, *PlosOne*, **9**, 1 (2014), https://doi.org/10.1371/journal.pone.0109545

40 S. S. Lucinaldo, C. B. L. Luciano, J. L. F. Francisco, S. S. Mateus, A. O. Josy *et al*., *Open Chem. J*., **13**, 801 (2015), https://doi.org/10.1515/chem-2015-0079

41 S. Boumchita, A. Lahrichi, Y. Benjelloun, S. Lairini, V. Nenov *et al*., *J. Mater. Environ. Sci*., **7**, 73 (2016)

42 T. Todorciuc, L. Bulgariu and V. I. Popa, *Cellulose Chem. Technol*., **49**, 439 (2015), https://www.cellulosechemtechnol.ro/pdf/CCT5-6(2015)/p.439-447.pdf

43 G. Crini, *Dyes Pigm*., **77**, 415 (2008), https://doi.org/10.1016/j.dyepig.2007.07.001

44 B. K. Nandi, A. Goswami and M. K. Purkait, *J. Hazard. Mater*., **161**, 387 (2009), https://doi.org/10.1016/j.jhazmat.2008.03.110

45 A. Afkhami and R. Moosavi, *J. Hazard. Mater*., **174**, 398 (2010), https://doi.org/10.1016/j.jhazmat.2009.09.066

46 A. A. Inyinbor, F. A. Adekola and G. A. Olatunji, *Water Resour. Ind*., **15**, 14 (2016), http://dx.doi.org/10.1016/j.wri.2016.06.001

[47] M. Arami, N. Y. Limaee, N. M. Mahmoodi and N. S. Tabrizi, *J. Colloid Interface Sci.*, **288**, 371 (2005), https://doi.org/10.1016/j.jcis.2005.03.020

[48] L. S. Krishna, A. S. Reddy, A. Muralikrishna, W. Y. WanZuhairi, H. Osman *et al.*, *Desalin. Water Treat.*, **56**, 2181 (2015), https://doi.org/10.1080/19443994.2014.958540

[49] V. S. Munagapati, V. Yarramuthi, Y. Kim, K. M. Lee and D. S. Kim, *Ecotoxicol. Environ. Saf.*, **148**, 601 (2018), https://doi.org/10.1016/j.ecoenv.2017.10.075
[53]

[50] A. Altinişik, E. Gür and Y. Seki, *J. Hazard. Mater.*, **179**, 658 (2010), https://doi.org/10.1016/j.jhazmat.2010.03.053

[51] E. O. Oyelude, J. A. M. Awudza and S. K. Twumasi, *J. Mater. Environ. Sci.*, **9**, 2087 (2018)

[52] Y. Uygun, H. Bayrak and H. Ozkan, *Turk. J. Chem.*, **37**, 812 (2013), https://doi.org/10.3906/kim-1212-66